New Mexico's COVID-19 Experience

Nicole R. Jackson, MD, MPH, Karen Zeigler, DO,* Mary Torrez, MD,* Yohsuke Makino, MD, PhD,†‡ Natalie L. Adolphi, PhD,* Sarah Lathrop, DVM, PhD,* Lauren Decker, MD,* Lauren Dvorscak, MD,* Lori Proe, DO,* Ian D. Paul, MD,* Ross Zumwalt, MD,* and Heather Jarrell, MD**

Abstract: The 2019 novel coronavirus disease (COVID-19) has spread worldwide, infiltrating, infecting, and devastating communities in all locations of varying demographics. An overwhelming majority of published literature on the pathologic findings associated with COVID-19 is either from living clinical cohorts or from autopsy findings of those who died in a medical care setting, which can confound pure disease pathology. A relatively low initial infection rate paired with a high biosafety level enabled the New Mexico Office of the Medical Investigator to conduct full autopsy examinations on suspected COVID-19–related deaths. Full autopsy examination on the first 20 severe acute respiratory syndrome coronavirus 2–positive decedents revealed that some extent of diffuse alveolar damage in every death due to COVID-19 played some role. The average decedent was middle-aged, male, American Indian, and overweight with comorbidities that included diabetes, ethanolism, and atherosclerotic and/or hypertensive cardiovascular disease. Macroscopic thrombotic events were seen in 35% of cases consisting of pulmonary thromboemboli and coronary artery thrombi. In 2 cases, severe bacterial coinfections were seen in the lungs. Those determined to die with but not of severe acute respiratory syndrome coronavirus 2 infection had unremarkable lung findings.

Key Words: COVID-19, forensic pathology, autopsy, Native American, New Mexico

(*Am J Forensic Med Pathol* 2021;42: 1–8)

Ever since their discovery in the 1960s, human coronaviruses have afflicted the world with pestilence, panic, and death.[1–4] Their infections range from mild, inconveniencing common colds to severe, debilitating and life-threatening respiratory infections as seen with the severe acute respiratory syndrome coronavirus (SARS-CoV), followed by the Middle East respiratory syndrome coronavirus, and now the novel 2019 coronavirus (SARS-CoV-2). Like other members of the coronaviridae, the novel 2019 coronavirus (COVID-19) emerged from an animal reservoir, this time in Wuhan, Hubei Province, China, and since December of 2019 has rapidly spread, infecting more than 33.5 million of the world's 7.8 billion inhabitants, resulting in the death of more than 1,000,000, and leading to morbidity in many of the recovered.[5,6] Since publicly infiltrating the United States in January 2020, more than 7.1 million have been infected with more than 200,000 resultant deaths.[7] Despite these large numbers, there have been relatively few published reports on the pathogenicity of SARS-CoV-2 based on disease findings in the dead. Initially compared with influenza, of which we know much about from autopsy studies, COVID-19 is proving to be a different beast, with much more remaining to be learned about its pathogenicity.[8,9]

The Office of the Medical Investigator (OMI) in Albuquerque, New Mexico, serves and has jurisdiction over the entire state, excluding federal and tribal land, investigating unnatural deaths as well as unattended natural deaths that occur outside of medical care, including deaths from COVID-19 infection. Its services are engaged in deaths occurring within New Mexico's American Indian Sovereign Nations, upon request, and extend to neighboring states when needed. By virtue of New Mexico having an initial slow infection rate and the OMI being a biosafety level 3 laboratory, the OMI was uniquely positioned at the onset of the pandemic to perform full autopsy examinations on all deaths occurring outside of medically managed care for which SARS-CoV-2 infection was suspected to play a role. By studying the lives and deaths of those with fatal COVID-19 infections, we hope to shed light on areas of potential interventions that can be of benefit to those still alive.

MATERIALS AND METHODS

A prospectively maintained database of all potential COVID-19 cases entering the OMI was constructed based on circumstances surrounding death including symptoms of fever, cough, shortness of breath, and general malaise as well as deaths occurring in areas with known high infection rates. Inclusion criteria were the first 20 deaths that tested positive for SARS-CoV-2, either antemortem or postmortem, and who underwent full autopsy examination. Decedents' viral status was assessed by postmortem nasopharyngeal and/or bilateral lung swabs with subsequent reverse transcription-polymerase chain reaction (RT-PCR) testing. Excluded were decedents who received inpatient medical care and those who underwent external autopsy examinations without dissection.

All autopsy examinations were performed in 1 of 4 isolation suites inside a biosafety level 3 laboratory by either a pathology resident, a forensic pathology fellow, and/or a board-certified forensic pathologist with appropriate personal protective equipment. Per standard operating procedure, decedents received full-body postmortem computed tomography (PMCT) imaging before autopsy examination using a Philips Brilliance Big Bore 16 Slice CT scanner with an 85-cm bore and a flat bariatric table, with Big Bore version 4.2 software. As a surrogate for assessing renal function, an electrolyte and glucose panel was performed on vitreous humor collected at the start of the examination. Toxicological testing for ethanol, illicit drugs, or commonly abused prescription and over-the-counter drugs was performed on peripheral blood, urine, or tissue samples at National Medical Services Labs. Samples for bacterial and viral testing were collected from the nasopharynx, heart blood, and bilateral lower lung lobes. At minimum, tissue samples from the lungs, heart, liver, kidneys, and brain were collected for microscopic examination, with the hippocampus and/or the cerebellar dentate nucleus preferentially sampled within the brain. For congruency in the interpretation of results, 2 fellows

Manuscript received October 15, 2020; accepted October 30, 2020.
From the *Office of the Medical Investigator, University of New Mexico, Albuquerque, New Mexico; †Department of Forensic Medicine, University of Tokyo, Tokyo; and ‡Department of Forensic Radiology and Imaging, Chiba University, Chiba, Japan.
The authors report no conflict of interest.
Reprints: Nicole R. Jackson, MD, MPH, Cook County Medical Examiner's Office, 2121 W. Harrison St, Chicago, IL 60612.
E-mail: Nicole.Jackson2@cookcountyil.gov.
Copyright © 2021 Wolters Kluwer Health, Inc. All rights reserved.
ISSN: 0195-7910/21/4201–0001
DOI: 10.1097/PAF.0000000000000664

Copyright © 2021 Wolters Kluwer Health, Inc. All rights reserved.

reviewed results from each included case including investigative reports, PMCT scans, histology, microbiology results, vitreous screens, and toxicology reports.

Primary measures of this study include the demographics of age, sex, and race, risk factors for acquisition of COVID-19 such as comorbidities, macroscopic and microscopic organ-specific findings, and the presence or absence of bacterial coinfection. Secondary measures of interest include locations of death, presenting symptoms, other significant autopsy findings, vitreous screen results, and toxicology findings.

As per 45 CFR 46, decedents are not considered human subjects and are not subject to institutional review board oversight.

RESULTS

Demographics

Between March 29 and June 8 of 2020, 162 decedents were transported to the OMI to determine if the etiology of their death included COVID-19. Representing a 12.35% case positivity rate,

TABLE 1. Demographics and Gross Organ Findings of the First 20 COVID-19–Positive Cases at the New Mexico OMI

Case	Age	Sex	Race	BMI	Location	Comorbidities	Right Lung	Left Lung	Heart	Brain	Gross Thrombi
1	40	M	W	24.57	Urban	Diabetes mellitus	850	680	370	1330	Absent
2	82	F	W	33.91	Urban	Hypertension	690	525	635	1195	Absent
3	58	F	AI	27.14	Reservation	Atherosclerotic cardiovascular disease, ethanolism	730	630	390	1065	Lung, small caliber
4	60	M	AI	34.73	Urban	Diabetes mellitus, ethanolism	1085	950	500	1375	Absent
5	60	M	AI	22.22	Homeless	Ethanolism	890	860	385	1275	Coronary artery
6	65	M	AI	28.28	Homeless	Atherosclerotic and hypertensive cardiovascular disease	870	615	765	1190	Lung, large caliber
7	62	M	AI	19.77	Rural	Atherosclerotic cardiovascular disease, chronic obstructive pulmonary disease, ethanolism	555	790	555	1300	Absent
8	34	M	AI	33.65	Rural	Long-standing dysphagia and shortness of breath	675	670	395	1495	Absent
9	29	F	AI	30.90	Rural	Ethanolism	460	415	310	1145	Absent
10	49	M	W	47.76	Urban	Asthma	1090	795	540	1460	Absent
11	70	M	AI	26.19	Rural	Atherosclerotic and hypertensive cardiovascular disease	970	515	450	1265	Absent
12	82	M	W	27.69	Urban	Atherosclerotic cardiovascular disease	805	540	560	1365	Bypass graft
13	62	M	AI	28.36	Rural, homeless	Ethanolism	1325	725	380	1350	Absent
14	50	M	AI	26.03	Rural, homeless	Diabetes mellitus, ethanolism	645	435	370	1100	Absent
15	40	M	AI	43.64	Unknown	Atherosclerotic cardiovascular disease	990	985	635	1535	Lung, small caliber
16	63	M	AI	27.51	Rural	Atherosclerotic and hypertensive cardiovascular disease, diabetes mellitus, end-stage renal disease	830	765	570	1400	Bypass graft
17	56	M	AI	28.54	Reservation	None known	970	600	530	1135	Lung, small caliber
18	39	M	AI	21.56	Rural, homeless	Ethanolism	855	760	365	1380	Absent
19	38	M	AI	26.20	Unknown	Ethanolism, drug abuse	755	1090	400	1315	Absent
20	62	M	AI	20.34	Reservation	Ethanolism, hypertensive cardiovascular disease	245	200	280	1265	Absent
Mean	55			28.95			814.25	677.25	469.3	1297	
Range	29–82			19.77–47.76			245–1325	200–1090	280–765	1065–1535	

Age measured in years. BMI measured in kilograms per meter squared. Organ weights measured in grams.

AI, American Indian; F, female; M, male. W, White.

© 2021 Wolters Kluwer Health, Inc. All rights reserved.

Copyright © 2021 Wolters Kluwer Health, Inc. All rights reserved.

20 of these tested positive for SARS-CoV-2 on postmortem sampling and underwent a full autopsy examination, with COVID-19 status resulted after examination. The average decedent was 55 years old (range, 29–82 years), male (n = 17), and American Indian (n = 16) and lived in a rural area (n = 15; Table 1).

Symptoms preceding death included shortness of breath (n = 10), cough (n = 6), fever (n = 6), malaise (n = 6), and chest pain or discomfort (n = 5), with rarer symptoms of backache, sore throat, chills, confusion, shaking, decreased oral intake, and abdominal symptoms of pain, vomiting, and diarrhea. One decedent was asymptomatic, whereas 5 were either homeless or living in isolation, and thus, information about circumstances surrounding death is lacking.

The average decedent was overweight with a body mass index (BMI) of 28.95 kg/m^2 (range, 19.77–47.76 kg/m^2). Although 2 morbidly obese decedents with BMIs of 43.64 and 47.76 kg/m^2 and 4 nonmorbidly obese decedents with an average BMI of 33.30 kg/m^2 mildly skewed this distribution, the remaining majority of decedents (n = 14) were slightly overweight with an average BMI of 25.31 kg/m^2 (Table 1). Comorbidities consisted of chronic ethanol abuse (n = 10), atherosclerotic cardiovascular disease (n = 7), hypertension (n = 5), diabetes mellitus (n = 4), asthma/chronic obstructive pulmonary disease (n = 2), end-stage renal disease (n = 1), chronic idiopathic shortness of breath (n = 1), and illicit drug abuse (n = 1).

PMCT Findings

Bilateral, ill-defined consolidations and/or mixed densities in either a diffuse or peripheral distribution were seen in a majority of decedents (n = 13; Fig. 1). Additional lung findings included pulmonary edema, large right pleural effusion (n = 1), and lobar consolidation (n = 2). Of note, 4 cases had unremarkable lung imaging.

Nonpulmonary imaging findings included cerebral edema, hepatomegaly, hepatic steatosis, decomposition changes, and evidence of atherosclerotic cardiovascular disease including varying amounts of calcification of the coronary arteries, aorta, and/or peripheral vascular disease.

Macroscopic Findings

Overall, lungs were edematous with an average weight of 814.25 g for the right lung (range, 245–1325 g) and 677.25 g for the left lung (200–1090 g). Pulmonary effusions were rare, with a 25-mL serosanguinous right pleural effusion in 1 case and a large 1200 mL serosanguinous right pleural effusion in another. Four cases demonstrated pulmonary thromboemboli: one of large-caliber and 3 with multiple subsegmental small-caliber emboli (Fig. 2). Adhesions, interstitial fibrosis, and frank purulence were rare events.

Most decedents had cardiomegaly with an average heart weight of 469.25 g (range, 280–765 g). Coronary thrombi were identified in 3 cases, 2 of which included a thrombus in a bypass graft (Fig. 2; Table 1). Additional common findings included hepatomegaly, hepatic steatosis and cirrhosis, granular kidneys, and cerebral edema.

Microscopic Findings

In most cases (n = 14), findings of diffuse alveolar damage (DAD) were identified, including early to well-established hyaline

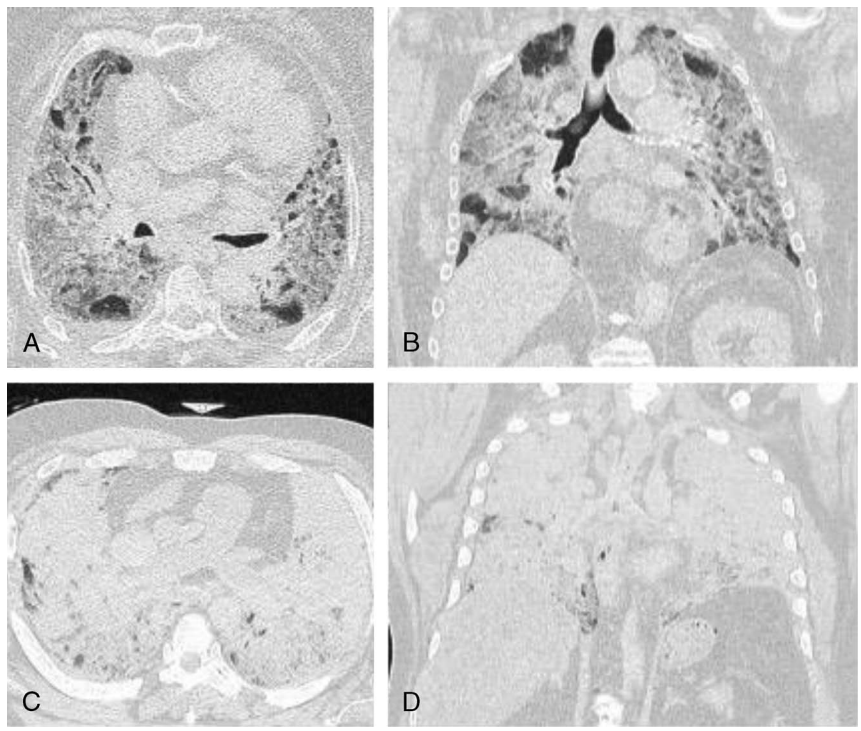

FIGURE 1. Postmortem computed tomography findings in rapidly fatal community cases of COVID-19. The lung windows of PMCT scans in 2 rapidly fatal COVID-19 cases. Case 2: an 82-year-old woman with a history of essential hypertension who reported severe cough, backache, chest pain, and sore throat before death. Bilateral, ill-defined, mixed densities in a diffuse distribution are demonstrated in the axial plane (A) and in the coronal plane (B). Case 4: a 60-year-old man with uncontrolled diabetes mellitus and chronic ethanol abuse who reported fever, cough, sore throat, dyspnea, and chest discomfort before death. Diffuse consolidations in both lungs are demonstrated in the axial plane (C) and in the coronal plane (D).

© 2021 Wolters Kluwer Health, Inc. All rights reserved.

Copyright © 2021 Wolters Kluwer Health, Inc. All rights reserved.

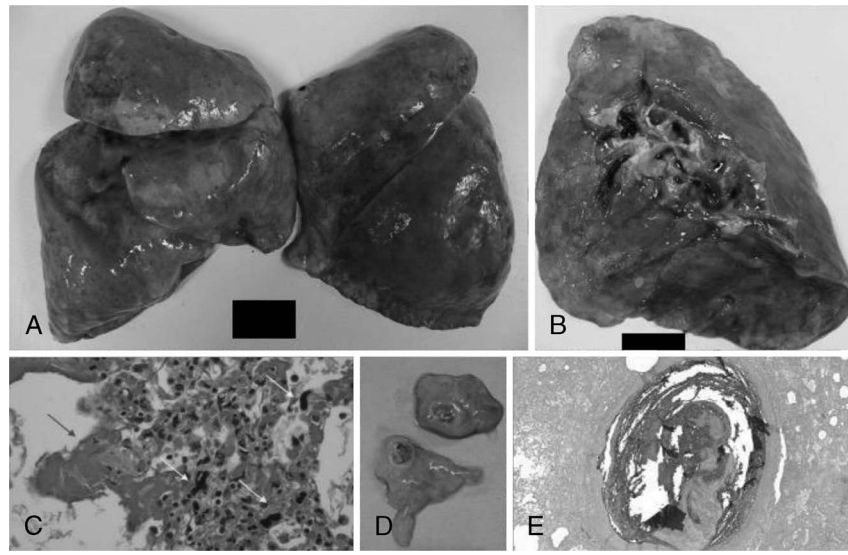

FIGURE 2. Gross and microscopic findings of cardiopulmonary thrombotic events identified at autopsy. Representative gross and microscopic findings in 5 decedents found to have macroscopic cardiopulmonary thrombotic events. A, Case 3: firm, slippery, edematous lungs with a combined weight of 1360 g. Sectioning revealed numerous small-caliber thrombi. B, Case 6: gross examination of an edematous 870-g right lung revealed large-caliber pulmonary thromboemboli in the superior branches of the pulmonary arteries. C, Case 3: in the microscopic correlate additionally seen are a predominance of interstitial megakaryocytes (yellow arrows), as well as hyaline membranes (blue arrow; H&E, original magnification ×40). D, Case 5: coronary artery thrombus of the left circumflex coronary artery seen in a homeless man. E, Case 6: microscopically, pulmonary thromboemboli correlated with layered blood components within the arterial lumina (Lines of Zhan), characteristic of antemortem formation (H&E, ×2).

membrane formation lining the alveolar walls, type II pneumocyte hyperplasia, intra-alveolar fibrin, and microthrombi with focal acute bronchitis (Fig. 3). In cases where gross pulmonary emboli were seen, interstitial megakaryocytes were pronounced (Fig. 2). Three cases demonstrated mild mixed interstitial inflammation, 2 demonstrated interstitial fibrosis, and 1 demonstrated an expanded interstitium with chronic inflammation. In 2 cases, in addition to hyaline membrane formation, there was dense neutrophilic inflammatory infiltrate involving the interstitium of the alveolar airspaces (Fig. 4).

Sections of cardiac ventricles revealed no significant inflammation or prominence of megakaryocytes. Similarly, microscopic examination of the liver, kidneys, and brain showed no significant inflammatory infiltrate or necrosis. In keeping with decedent histories, hepatic steatosis and cirrhosis were common findings, as were focal global glomerulosclerosis and nephrosclerosis.

Ancillary Studies

Infectious Disease Testing

The 2019 novel coronavirus (SARS-CoV-2) was detected in swabs of either the lungs and/or the nasopharynx by TaqPath COVID-19 Combo RT-PCR in all 20 cases, with 17 cases demonstrating concordant positivity between all sites of collection. The 3 outlying cases included an isolated positive right lung culture in someone who died of a fentanyl overdose, an isolated positive right lung culture in someone who died of atherosclerotic and hypertensive cardiovascular disease, and positive nasopharyngeal and right lung cultures in someone who died of complications of chronic ethanol abuse. Influenza A and B were not detected by real-time RT-PCR in any case.

In 2 cases, there was significant bacterial growth. The first case (case 13) grew *Streptococcus pneumoniae* from the heart blood and both lungs in concordance with microscopic findings of intra-alveolar aggregates of polymorphonuclear leukocytes associated with diplococci. The second case (case 19) also grew *S. pneumoniae* and exhibited a dense neutrophilic inflammatory infiltrate (Fig. 4).

Vitreous Screen and Toxicology

Testing of the vitreous fluid for disturbances in electrolytes and glucose was performed on 13 cases, 8 of which were within normal limits. Two cases of diabetics in ketoacidosis revealed profound hyperglycemia with glucose levels of 509 and 886 mmol/L, both of which had acetone detected on toxicology. A dehydration pattern was seen in 1 case, and severe elevations in vitreous urea nitrogen and creatinine were seen in a decedent with known chronic renal failure. In only 1 case was renal failure unexpectedly seen, with vitreous urea nitrogen of 58 mmol/L and creatinine of 3.4 mmol/L.

Postmortem toxicology was negative in 10 of the 17 cases tested. In the remaining 7 cases, 3 were acutely intoxicated with ethanol, 1 with methamphetamine, and 1 with fentanyl. One ethanol level was considered lethal at 0.381 g/dL. As previously stated, acetone was detected in 2 decedents.

DISCUSSION

The population in New Mexico that died of COVID-19 outside of medical care tended to be middle-aged Native American men residing in rural areas and reservations, mirroring a disparity of disease burden seen on both the state and national level.[10] Common comorbidities included chronic ethanol abuse with cirrhosis and/or hepatic steatosis, diabetes mellitus, atherosclerotic cardiovascular disease, hypertension, and obesity with environmental risk factors that included homelessness and cohabitation with known COVID-19–positive individuals. Indigenous communities in America have higher rates of cardiovascular disease, obesity, diabetes mellitus, and tobacco use as compared with the remaining national population, factors associated with poorer outcomes in

© 2021 Wolters Kluwer Health, Inc. All rights reserved.

Copyright © 2021 Wolters Kluwer Health, Inc. All rights reserved.

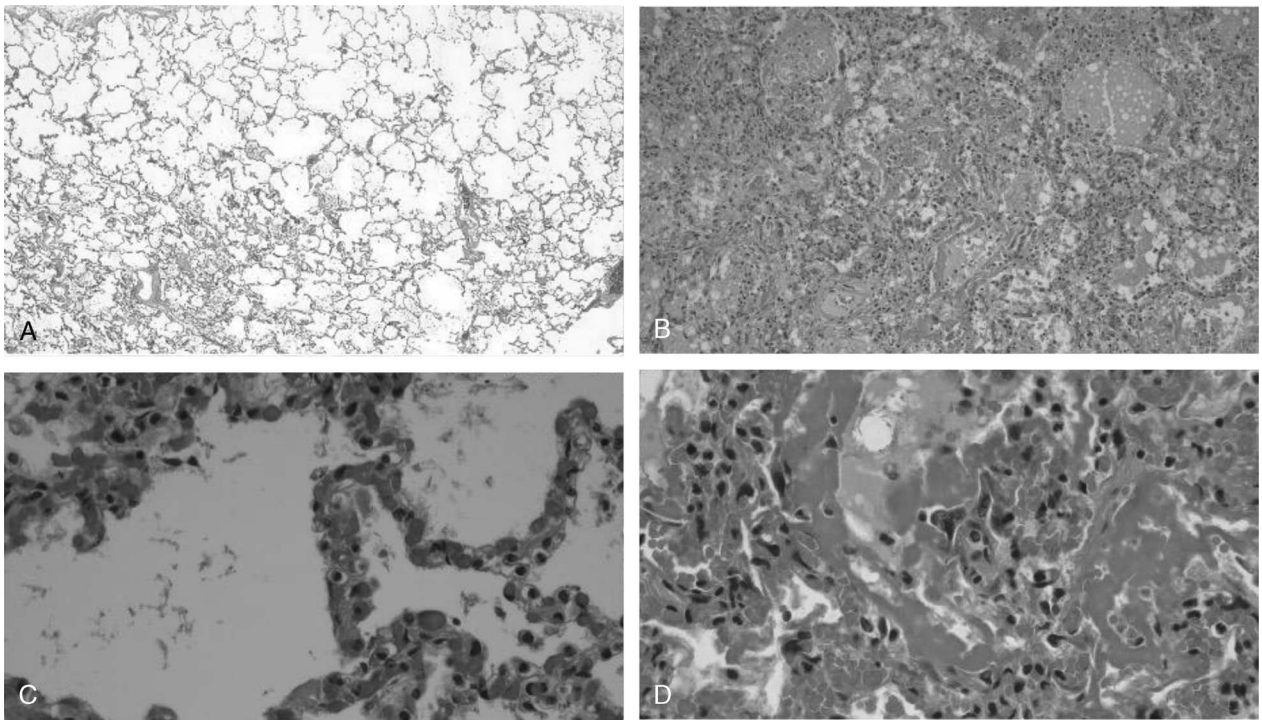

FIGURE 3. Comparison of microscopic lung findings in asymptomatic carriers with those with aggressive, symptomatic infections. Postmortem lung sections with no significant histology findings in decedents whose deaths were attributed to intoxication as compared with deaths attributed to COVID-19 infection, which are characterized by DAD. A, Case 8: low-power view of a decedent who died of fentanyl toxicity who incidentally tested positive for COVID-19 (H&E, original magnification ×2). B, Case 7: low-power view of the lungs of a chronic alcoholic who reported fever, cough, and feeling unwell before collapsing at home demonstrating congested intra-alveolar airspaces containing hyaline membranes, pulmonary edema, type II pneumocytes hyperplasia, macrophages, and fibrin (H&E, ×10). C, Case 9: high-power view of the lungs of a decedent who died of acute ethanol intoxication but tested positive for COVID-19 (H&E, ×40). D, Case 4: high-power view of extensive DAD with hyaline membrane formation, type II pneumocyte hyperplasia, pulmonary edema in a man with uncontrolled diabetes mellitus and chronic ethanolism who reported fever, cough, sore throat, dyspnea, and chest pain before death (H&E, ×40).

COVID-19.[11–13] Furthermore, numerous cultural practices and societal norms are attributed to the higher COVID-19–related morbidity and mortality seen in this community, including multiple generations sharing a household, reduced access to running water and quality healthy food, indoor air pollution related to meal preparation, high rates of chronic and undiagnosed disease, and reduced access to medical care.[14] In particular, diabetes has a prevalence in this community that is nearly 3 times as high as that of non-Hispanic Whites in America. Combined with poor access to medical care and quality food, it is a disease that is not uncommonly poorly controlled in American Indians.[12] Two of 4 decedents with known diabetes were in ketoacidosis at the time of death, 1 of which had a recent hemoglobin A_{1c} value of 18%. Furthermore, the most severe lung pathology seen in the cohort was in a diabetic. This represents an opportunity for targeted community-based public health campaigns designed to address the obstacles to achieving good blood glucose control to save lives from COVID-19 and from other diabetes complications.

In disease emergence on any scale, elucidation of underlying pathology—morbidity and mortality —is imperative to saving lives, with autopsy examination being the criterion standard for understanding the pathophysiology of disease.[15,16] Although there is a multitude of literature on COVID-19 and more than 1 million deaths worldwide, there are few published studies on postmortem examination findings. To date, only 15 peer-reviewed studies have been published from autopsies conducted on COVID-19 deaths in the United States, some of which limited their findings to only 1 or 2 organs, representing 114 fatal cases spanning 7 states (Table 2).[17–31] Of these, only 2 recount the experience of 6 people who died within the community outside of a medical care setting. Because some of SARS-CoV-2–identified pathologic findings can be iatrogenically introduced, delineation by comparison of community with hospital COVID-19–associated deaths is imperative. Similar to both hospital- and community-based series and to other members of the coronaviridae, the lungs of decedents in which COVID-19 contributed to death all exhibited features of DAD by microscopy, with varying degrees of hyaline membrane formation, type II pneumocyte hyperplasia, intra-alveolar fibrin, and pulmonary edema. Unlike hospital-based deaths, pulmonary microthrombi and megakaryocyte prominence were relatively rare events associated with macroscopic pulmonary thromboemboli. By comparison, deaths in this series that were attributed to intoxication without significant contribution from SARS-CoV-2 infection lacked these microscopic findings and represent the lungs of asymptomatic community infections. Even in these asymptomatic cases, swabs of not only the nasopharynx but also the lower lung lobes were positive for SARS-CoV-2 detection.

Notably, 2 decedents had lungs that were coinfected with *S. pneumoniae*, the most common cause of community-acquired pneumonia and the most commonly detected bacterial coinfection or superinfection in viral pneumonias.[32–35] Each was consolidated by PMCT and palpation, exhibiting frank purulence, and microscopically displayed sheets of neutrophils, with one showing numerous diplococci on hematoxylin and eosin (H&E) staining. In one of these cases (case 13), early features of DAD could be seen on microscopy; however, in the other case (case 19), the neutrophilic response was

© 2021 Wolters Kluwer Health, Inc. All rights reserved.

Copyright © 2021 Wolters Kluwer Health, Inc. All rights reserved.

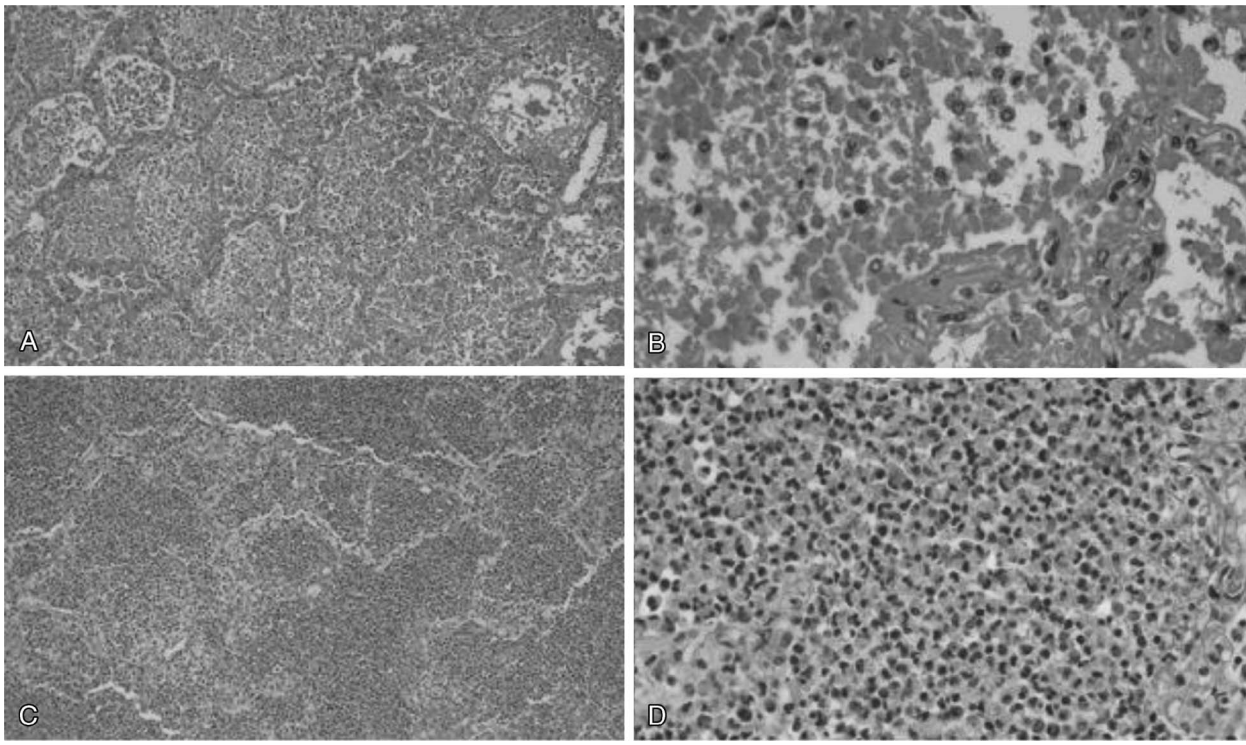

FIGURE 4. Two cases of coinfection with SARS-CoV-2 and *S. pneumoniae*. In 2 cases, decedents were positive both for COVID-19 infection and for a concomitant bacterial lung infection with *S. pneumoniae*. A, Case 13: diffuse intra-alveolar neutrophils with hyaline membrane formation (H&E, original magnification ×10). B, Case 13: intra-alveolar neutrophils and hyaline membranes with associated diplococci, intra-alveolar hemorrhage and fibrin, and coagulative necrosis (H&E, ×40). C, Case 19: sheets of intra-alveolar neutrophils (H&E, ×10). D. Case 19: sheets of neutrophils with coagulative necrosis (H&E, ×40).

brisk and underlying lung pathology was masked. It is unsurprising that this finding is rare in other series, as most samples consisted of patients who received broad-spectrum antibiotics. Of note, one non–peer-reviewed article also mentions several cases of superimposed acute pneumonia but does not report involved microorganisms or histologic finding.[36] SARS-CoV-2 infection seems to have a low rate of concomitant bacterial lung infection, which is dissimilar to influenza and similar to other coronaviruses.[37]

Although myocarditis can be associated with viral infections, inflammation of the heart was not seen congruent with all published autopsy studies, save one.[30] However, the rare event of coronary artery thrombus was identified in 3 of our decedents: 2 in their bypass grafts and 1 in a native vessel. Another article reported a similar finding of myocardial venous thrombosis.[28] These 3 cases in conjunction with 4 cases with pulmonary thromboemboli represent a 35% case rate of thrombotic sequelae, strengthening the hypothesis that COVID-19 promotes a hypercoagulable state, supporting the use of antiplatelet agents for therapeutic intervention.

No significant findings related to infection or thrombotic events were identified in remaining organs examined. Although one vitreous electrolyte and glucose screen unexpectedly revealed renal failure, microscopically the kidneys showed no evidence of acute tubular necrosis. Neither areas of hypoxic-ischemic changes nor significant inflammation was seen in the brain. Unlike another study, megakaryocytes were restricted to the lungs.[28]

This study remains limited in that it consists of a relatively small sample size that, like prior studies, may be underpowered to detect true relationships between COVID-19 and disease processes. Importantly, this series speaks exclusively to the experience of those with COVID-19 who did not receive significant medical intervention and died. Based on public health statistics, it is known that most infections are not fatal, and thus, pathologic features represented here are likely more severe than those seen in the average infection. This is reaffirmed by those decedents who tested positive at autopsy but were found to die with, not of, SARS-CoV-2 infection and who had unremarkable lungs, histologically and by PMCT. The histopathology of those who reach medical care in time likely lies somewhere between the 2. Likewise, this report is limited to the state of New Mexico's experience, which might not be generalizable to the rest of the country or to the rest of the world owing to possible underlying genetic variance in a population that includes a large portion of individuals of Native American descent. In addition, because of overwhelmed central clinical laboratories, viral studies were reduced to assessment only for coinfection with influenza, limiting the assessment of coinfection with other respiratory pathogens that have been reported clinically.[38] To address the aforementioned limitations, further studies are needed: both additional smaller case reports and series that can be aggregated into systematic reviews and meta-analyses, as well as larger multi-institutional studies.

CONCLUSIONS

This cohort represents the largest series in the world of autopsy findings in COVID-19 in the absence of hospitalization or long-term medical facilities. Rapidly fatal infections were predominantly seen in a middle-aged male American Indians residing in rural areas with histories that included ethanolism, diabetes, and

© 2021 Wolters Kluwer Health, Inc. All rights reserved.

Copyright © 2021 Wolters Kluwer Health, Inc. All rights reserved.

TABLE 2. Comparison of Peer-Reviewed Published US Findings in Autopsies of Fatal COVID-19 Cases

	Publication Date	Authors	City	State	Setting	n	Mean Age, y	Organs Studied and/or Reported	Major Histologic Findings
1	04/10/2020	Barton et al[17]	Oklahoma City	OK	Community	2	59.5	Lungs, heart, kidneys, liver, brain	DAD in only the COVID death
2	04/15/2020	Yan et al[18]	San Antonio	TX	Hospital	1	44	Lungs, heart, kidney (by biopsy)	DAD, pulmonary infarct
3	04/21/2020	Paniz-Mondolfi et al[19]	New York	NY	Hospital	1	74	Brain	Viral particles in endothelial cells
4	04/28/2020	Konopka et al[20]	Ann Arbor	MI	Hospital	1	37	Lungs	DAD and mucus plugs
5	05/07/2020	Buja et al[21]	Houston	TX	Mixed	3	48	Lungs, heart, kidneys, liver, spleen	DAD, microthrombi common but not universal, PEs common
6	05/21/2020	Ackermann et al[22]	Boston	MA	Hospital	7	78.4	Lungs	Vascular thrombosis with microangiopathy, angiogenesis, endothelialitis
7	05/24/2020	Reichard et al[23]	Rochester	NY	Hospital	1	71	Brain	Lack of typical features of viral and postviral encephalitides
8	05/27/2020	Fox et al[24]	New Orleans	LA	Hospital	10	63	Lungs and heart	Thrombotic microangiopathy limited to the lungs, lack of secondary lung infection
9	05/2020	Martines et al[25]	—	WA	Hospital	8	73.5	Lungs	Varying DAD with no correlation with symptom duration
10	06/15/2020	Konopka et al[26]	Ann Arbor	MI	Community	4	53	Lungs	DAD
11	06/19/2020	Schaefer et al[27]	Boston	MA	Hospital	7	66	Lungs	DAD with pneumocyte hyperplasia
12	06/25/2020	Rapkiewicz et al[28]	New York	NY	Hospital	7	57.4	Lungs, heart, kidneys, liver, bone	Megakaryocytes in the vascular beds of lungs and heart, 2 cases of myocardial venous thrombosis
13	07/02/2020	Sauter et al[29]	New York	NY	Hospital	8	57.5	Lungs	Thrombi, microthrombi
14	07/16/2020	Bradley et al[30]	Seattle, Everett	WA	Hospital	14	73.5	Lungs, heart, kidneys, liver, brain	One case of lymphocytic myocarditis
15	09/02/2020	De Michele et al[31]	New York	NY	Hospital	40	71.5	Lungs	Acute lung injury and nonacute lung injury patterns found
Mean						7.6	61.8		

n, sample size; PE, pulmonary emboli.

atherosclerotic and/or hypertensive cardiovascular disease. Our findings were largely consistent with those of other groups including the pervasiveness of histologic findings of DAD and hypercoagulability. Superimposed deadly bacterial pneumonia with *S. pneumoniae* and poor outcomes in diabetic patients were additional findings. Asymptomatic carriers who died of intoxications had histologically unremarkable lungs despite positive nasopharyngeal and/or lung swabs. Not seen were fatal pediatric infections, myocarditis, or encephalitis.

REFERENCES

1. Tyrrell DA, Bynoe ML. Cultivation of a novel type of common-cold virus in organ cultures. *Br Med J*. 1965;1(5448):1467–1470.
2. Hamre D, Procknow JJ. A new virus isolated from the human respiratory tract. *Proc Soc Exp Biol Med*. 1966;121(1):190–193.
3. McIntosh K, Dees JH, Becker WB, et al. Recovery in tracheal organ cultures of novel viruses from patients with respiratory disease. *Proc Natl Acad Sci U S A*. 1967;57(4):933–940.
4. Almeida JD, Tyrrell DA. The morphology of three previously uncharacterized human respiratory viruses that grow in organ culture. *J Gen Virol*. 1967;1(2):175–178.
5. Zhu N, Zhang D, Wang W, et al, China Novel Coronavirus Investigating and Research Team. A novel coronavirus from patients with pneumonia in China, 2019. *N Engl J Med*. 2020;382(8):727–733.
6. World Health Organization. WHO coronavirus disease (COVID-19) dashboard. Available at: https://covid19.who.int/. Accessed September 30, 2020.
7. Centers for Disease Control and Prevention. CDC COVID data tracker—maps, charts, and data provided by the CDC. Available at: https://covid.cdc.gov/covid-data-tracker/#cases. Accessed September 30, 2020.
8. Cox MJ, Loman N, Bogaert D, et al. Co-infections: potentially lethal and unexplored in COVID-19. *Lancet Microbe*. 2020;1(1):e11.

© 2021 Wolters Kluwer Health, Inc. All rights reserved.

Copyright © 2021 Wolters Kluwer Health, Inc. All rights reserved.

9. European Centre for Disease Prevention and Control. Evidence from autopsies on the pathogenesis and pathological findings of the 2009 pandemic influenza A (H1N1)—implications for clinical care and disease burden, February 2011. Available at: https://www.ecdc.europa.eu/en/news-events/evidence-autopsies-pathogenesis-and-pathological-findings-2009-pandemic-influenza-ah1n1. Accessed September 4, 2020.
10. New Mexico Department of Health COVID-19 in New Mexico. Statewide race/ethnicity breakdown. Available at: https://cvprovider.nmhealth.org/public-dashboard.html. Accessed September 30, 2020.
11. Martinez-Maldonado M. Hypertension in Hispanics, Asians and Pacific-Islanders, and Native Americans. *Circulation*. 1991;83(4):1467–1469.
12. Poudel A, Zhou JY, Story D, et al. Diabetes and associated cardiovascular complications in American Indians/Alaskan Natives: a review of risks and prevention strategies. *J Diabetes Res*. 2018;2018:2742565.
13. Centers for Disease Control and Prevention, National Vital Statistics Reports, 2018. Table 19. Current cigarette smoking among adults aged 18 and over, by selected characteristics: United States, average annual, selected years 1990–1992 through 2015–2017. Available at: https://www.cdc.gov/nchs/data/hus/2018/019.pdf. Accessed June 2020.
14. Kakol M, Upson D, Sood A. Susceptibility of Southwestern American Indian tribes to coronavirus disease 2019 (COVID-19) [published online April 18, 2020]. *J Rural Health*. doi:10.1111/jrh.12451.
15. Sarode VR, Datta BN, Banerjee AK, et al. Autopsy findings and clinical diagnoses: a review of 1,000 cases. *Hum Pathol*. 1993;24(2):194–198.
16. Roosen J, Frans E, Wilmer A, et al. Comparison of premortem clinical diagnoses in critically iII patients and subsequent autopsy findings. *Mayo Clin Proc*. 2000;75(6):562–567.
17. Barton LM, Duval EJ, Stroberg E, et al. COVID-19 autopsies, Oklahoma, USA. *Am J Clin Pathol*. 2020;153(6):725–733.
18. Yan L, Mir M, Sanchez P, et al. Autopsy report with clinical pathological correlation [published online May 18, 2020]. *Arch Pathol Lab Med*. 10.5858/arpa.2020-0217-SA.
19. Paniz-Mondolfi A, Bryce C, Grimes Z, et al. Central nervous system involvement by severe acute respiratory syndrome coronavirus-2 (SARS-CoV-2). *J Med Virol*. 2020;92(7):699–702.
20. Konopka KE, Wilson A, Myers JL. Postmortem lung findings in a patient with asthma and coronavirus disease 2019. *Chest*. 2020;158(3):e99–e101.
21. Buja LM, Wolf DA, Zhao B, et al. The emerging spectrum of cardiopulmonary pathology of the coronavirus disease 2019 (COVID-19): report of 3 autopsies from Houston, Texas, and review of autopsy findings from other United States cities. *Cardiovasc Pathol*. 2020;48:107233.
22. Ackermann M, Verleden SE, Kuehnel M, et al. Pulmonary vascular endothelialitis, thrombosis, and angiogenesis in COVID-19. *N Engl J Med*. 2020;383(2):120–128.
23. Reichard RR, Kashani KB, Boire NA, et al. Neuropathology of COVID-19: a spectrum of vascular and acute disseminated encephalomyelitis (ADEM)–like pathology. *Acta Neuropathol*. 2020;140(1):1–6.
24. Fox SE, Akmatbekov A, Harbert JL, et al. Pulmonary and cardiac pathology in African American patients with COVID-19: an autopsy series from New Orleans. *Lancet Respir Med*. 2020;8(7):681–686.
25. Martines RB, Ritter JM, Matkovic E, et al, COVID-19 Pathology Working Group. Pathology and pathogenesis of SARS-CoV-2 associated with fatal coronavirus disease, United States. *Emerg Infect Dis*. 2020;26(9):2005–2015.
26. Konopka KE, Nguyen T, Jentzen JM, et al. Diffuse alveolar damage (DAD) resulting from coronavirus disease 2019 infection is morphologically indistinguishable from other causes of DAD. *Histopathology*. 2020;77(4):570–578.
27. Schaefer IM, Padera RF, Solomon IH, et al. In situ detection of SARS-CoV-2 in lungs and airways of patients with COVID-19. *Mod Pathol*. 2020;33:2104–2114.
28. Rapkiewicz AV, Mai X, Carsons SE, et al. Megakaryocytes and platelet-fibrin thrombi characterize multi-organ thrombosis at autopsy in COVID-19: a case series. *EClinicalMedicine*. 2020;24:100434.
29. Sauter JL, Baine MK, Butnor KJ, et al. Insights into pathogenesis of fatal COVID-19 pneumonia from histopathology with immunohistochemical and viral RNA studies. *Histopathology*. 2020;77(6):915–925.
30. Bradley BT, Maioli H, Johnston R, et al. Histopathology and ultrastructural findings of fatal COVID-19 infections in Washington State: a case series. *Lancet*. 2020;396(10247):320–332.
31. De Michele S, Sun Y, Yilmaz MM, et al. Forty postmortem examinations in COVID-19 patients. *Am J Clin Pathol*. 2020;154(6):748–760.
32. Morris DE, Cleary DW, Clarke SC. Secondary bacterial infections associated with influenza pandemics. *Front Microbiol*. 2017;8:1041.
33. Brundage JF. Interactions between influenza and bacterial respiratory pathogens: implications for pandemic preparedness. *Lancet Infect Dis*. 2006;6(5):303–312.
34. Avadhanula V, Wang Y, Portner A, et al. Nontypeable Haemophilus influenzae and *Streptococcus pneumoniae* bind respiratory syncytial virus glycoprotein. *J Med Microbiol*. 2007;56(Pt 9):1133–1137.
35. Avadhanula V, Rodriguez CA, Devincenzo JP, et al. Respiratory viruses augment the adhesion of bacterial pathogens to respiratory epithelium in a viral species- and cell type–dependent manner. *J Virol*. 2006;80(4):1629–1636.
36. Bryce C, Grimes Z, Pujadas E, et al. Pathophysiology of SARS-Cov-2: targeting of endothelial cells renders a complex disease with thrombotic microangiopathy and aberrant immune response. The Mount Sinai COVID-19 autopsy experience. *Med Rxiv*. 2020.
37. Langford BJ, So M, Raybardhan S, et al. Bacterial co-infection and secondary infection in patients with COVID-19: a living rapid review and meta-analysis. *Clin Microbiol Infect*. 2020;26(12):1622–1629.
38. Kim D, Quinn J, Pinsky B, et al. Rates of co-infection between SARS-CoV-2 and other respiratory pathogens. *JAMA*. 2020;323(20):2085–2086.

© 2021 Wolters Kluwer Health, Inc. All rights reserved.

Copyright © 2021 Wolters Kluwer Health, Inc. All rights reserved.